JOURNAL OF MATERIALS SCIENCE 21 (1986) 2430–2434

A kinetic study of the silver–mercury contact reaction

K. H. LEE, M. C. SHIN, J. Y. LEE
Department of Materials Science and Engineering, Korea Advanced Institute of Science and Technology, PO Box 131, Chongryang, Seoul, Korea

The solid–liquid diffusion couple technique was employed to determine the interdiffusion coefficient of the gamma phase in the Ag–Hg contact reaction. Diffusion coefficients were calculated with the aid of an equation given by Wagner. The composition range of the gamma phase was determined to be between 55.3 and 57.5 at% by electron microprobe analysis, and values for the average interdiffusion coefficient of the gamma phase were found to be $D_{av}(\text{cm}^2\,\text{sec}^{-1}) = 3.181 \times 10^{-5} \exp(-32\,539(\text{J}\,\text{mol}^{-1})/RT)$ in the temperature range 40 to 115° C. The amalgamation reaction between silver and liquid mercury proceeded with the formation of gamma phase and a solid solution of Ag–Hg. The growth of gamma phase followed a parabolic rate law. The penetration of liquid mercury into grain boundary of the gamma phase caused the gamma to be crumbled off. The possibility of short-circuit diffusion is discussed.

1. Introduction

The reaction between silver and liquid mercury is of interest to dentists and material scientists for understanding the basic nature of the amalgamation reaction in dental amalgam. The dental amalgamation reaction is the reaction between alloy powders of Ag–Sn–Cu–Zn and liquid mercury at human body temperature. There have been several kinetic researches on dental amalgam. Malhotra *et al.* [1] measured the volume diffusion coefficient of mercury in Ag_3Sn by X-ray energy-dispersive spectrometry and obtained coefficients of the order of $10^{-13}\,\text{cm}^2\,\text{sec}^{-1}$ at 37° C. Okabe *et al.* [2] evalulated the volume and grain-boundary diffusion coefficients of mercury in Ag_3Sn by the residual-activity method. Volume diffusion coefficients were of the order of $10^{-11}\,\text{cm}^2\,\text{sec}^{-1}$, and grain-boundary coefficients were of the order of $10^{-3}\,\text{cm}^2\,\text{sec}^{-1}$ at 50° C.

Although the kinetic study of mercury in silver plays an important role in understanding the amalgamation process, relatively little work has been done in this field. Sawatzky and Jaumot [3] studied this system in the temperature range 650 to 950° C. The extrapolated volume diffusion coefficient of mercury in silver was of the order of $10^{-28}\,\text{cm}^2\,\text{sec}^{-1}$ at 37° C. This value was much lower than that of mercury in Ag_3Sn. Suprinick [4] studied an Ag–Hg reaction to relate this reaction to the properties of dental amalgam, but he did not give detailed kinetic data for the Ag–Hg reaction. This work was thus undertaken to obtain more accurate diffusion data of Hg–Ag at lower temperatures, and to understand the basic reaction between silver and liquid mercury.

2. Experimental procedure

The reaction kinetics between silver and liquid mercury were studied by the solid/liquid diffusion couple technique in a Teflon reaction cell. For sample preparation, silver discs, 0.75 cm diameter × 0.2 cm, were cut by a spark erosion machine (Servomet SMD, London, UK) from a cold-rolled silver sheet, nominal purity 99.9%, and polished to a final grit of 0.05 μm alumina. All discs were annealed at 700° C for 30 min in a hydrogen atmosphere. Immediately prior to placing the disc in mercury contained in a Teflon capsule (Fig. 1) the disc was ion-sputtered in an argon plasma sputter (Eiko Ion Coater IB-3, Tokyo, Japan) to remove the surface impedance layer of the disc. The disc was then mounted in a Teflon reaction cell with its polished side in contact with 30 ml mercury (nominal purity 99%), and tightly closed with a screwed brass cap in an argon atmosphere. To wet the surface of the silver disc with liquid mercury efficiently, the reaction cell was triturated in a conventional dental amalgamator (S.S.White Capmaster) for 3 min. The individual reaction cells were heated in silicone-oil baths at preset temperatures and times. After the heat treatment, the disc was taken out of the capsule. The liquid mercury retained on the silver disc was suctioned and removed by a modified syringe with a rubber-coated flat needle.

After removal of mercury the discs were immediately mounted for observation in a scanning electron microscope (ISI SEM DS-130). After the observation of the disc surface in the SEM, the samples were taken out of the SEM to prepare them for the measurement of reaction product layer thickness. The discs were sectioned by a low-speed diamond cutter (Buehler Isomet), cold-mounted with graphite powder mixed with a rapid-curing resin to be conductive in the SEM, ground and polished, and etched with 4 wt % iodine in ethyl alcohol followed by 5 wt % sodium thiosulphate in water [5].

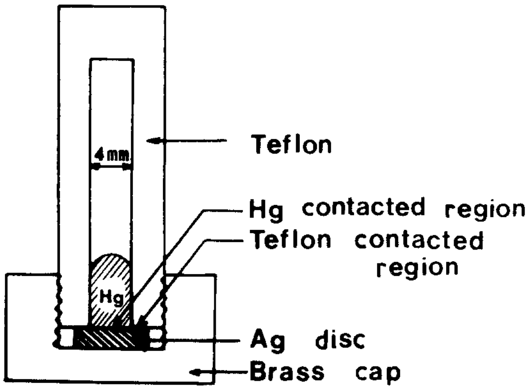

Figure 1 A schematic view of the reaction cell.

The layer thickness was measured using a digital filar micrometer on Vickers microhardness tester (Tukon Microhardness Tester) and confirmed by SEM with a microprobe (EDAX WEDAX III). To identify the reaction products, the full quantitative programme (COR 2) of the electron probe microanalyser (EPMA) was used, and standards for microanalysis were HgS (Cinnabar, 13.78 wt % S, 86.22 wt % Hg) for mercury, and pure silver (99.99%) for silver. The accelerating voltage was 30 kV and $\mathrm{Ag}L_1^\alpha$ and $\mathrm{Hg}L_1^\alpha$ radiations were employed. The reported compositions are accurate within 0.5 at %.

3. Results

The reaction products in the silver–mercury contact reaction agreed substantially with the phase diagram (Fig. 2) published by Hansen [6]. Gamma phase was found in the surface of the silver disc over the range of temperature used in this study. Fig. 3 shows the gamma crystals surrounded by the remaining liquid mercury in the Ag–Hg diffusion couple, after annealing at 115° C for 65 h and 15 min after mounting in the SEM. After 5 h in the SEM, the remaining liquid mercury was fully evaporated and sharply faceted polyhedral crystals Region A) and flat crystals (Region B) were observed as in Fig. 4. They were all identified as gamma crystals by the electron microprobe. The composition range of these crystals was about 55.3 to 57.5 at % Hg, which substantially coincides with the data of Hansen [6].

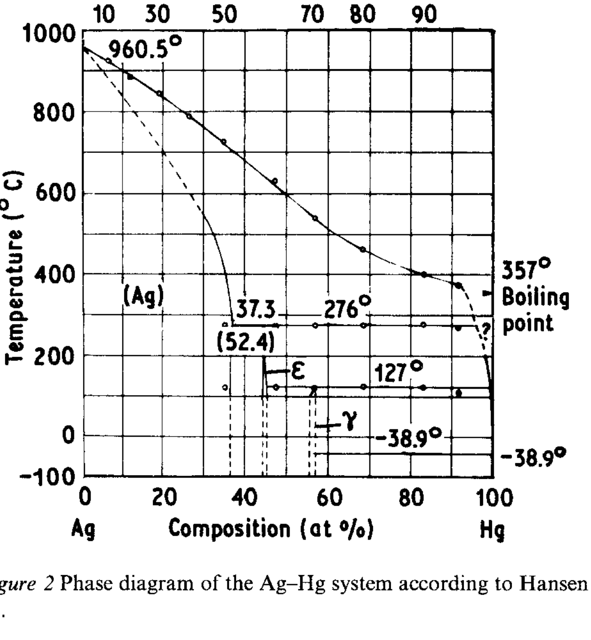

Figure 2 Phase diagram of the Ag–Hg system according to Hansen [6].

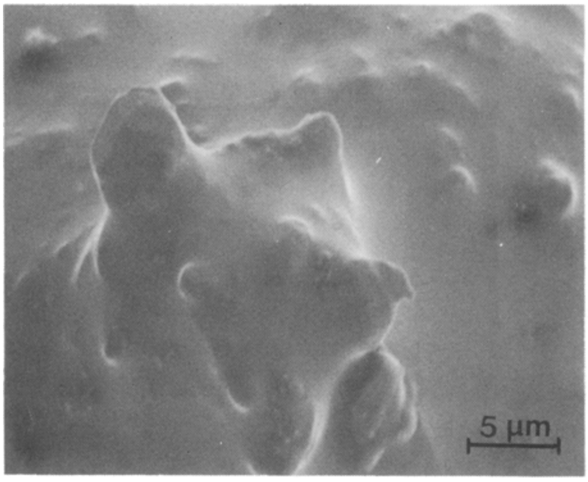

Figure 3 SEM micrograph taken 15 min after mounting in the SEM, showing the surface of an amalgamated silver disc often annealing at 115° C for 65 h. Note that reaction products are surrounded by the remaining liquid mercury and they have sharply faceted faces.

It is interesting to note the differences of crystal size and shape between the mercury-contacted region (A in Fig. 4) and the Teflon-masked region (B in Fig. 4) on the silver disc surface. The sharply faceted crystals in Region A could grow freely in liquid mercury, but the flat and tiny crystals in Region B could not grow freely due to the restriction of the adjacent Teflon wall. The crystal size was also affected by the reaction temperature. The size of crystals in Fig. 4b annealed at 90° C was larger than that of Fig. 4b annealed at 60° C for the same reaction time.

Fig. 5 shows a sectional view of the Ag–Hg coupled mounted in graphite mixed with cold-mounting resin. The sample was etched with 4 wt % iodine in ethyl alcohol followed by 5 wt % sodium thiosulphate in water. The X-ray line scan (Fig. 5b) and the point analysis by electron probe show that the first layer of the reaction product was gamma crystals. During the growth of this crystal layer, the liquid mercury penetrated the grain boundary of this layer. So pieces of this phase crumbled off and were spread in the liquid mercury as shown in the mercury-contacted region of Figs. 5a and 6a. At higher temperatures these phenomena were more pronounced.

To determine the reaction rate, the square of the thickness of the growing alloy layer (gamma phase) is plotted against time in Fig. 7. The thickness of the gamma phase identified by EPMA is measured with reference to the unreacted zone in contact with the Teflon frame to include the crumbled-off area. The growth rate follows a parabolic rate law, which indicates that the process of the reaction is controlled by diffusion. Wagner [7] has derived an equation for the interdiffusion coefficients accounting for the change in the partial molar volume. The equation is an extension of the Sauer and Freise form of Boltzmann and Matano's analysis to the multiphase diffusional growth of an intermetallic compound layer. This method provides a mean diffusivity

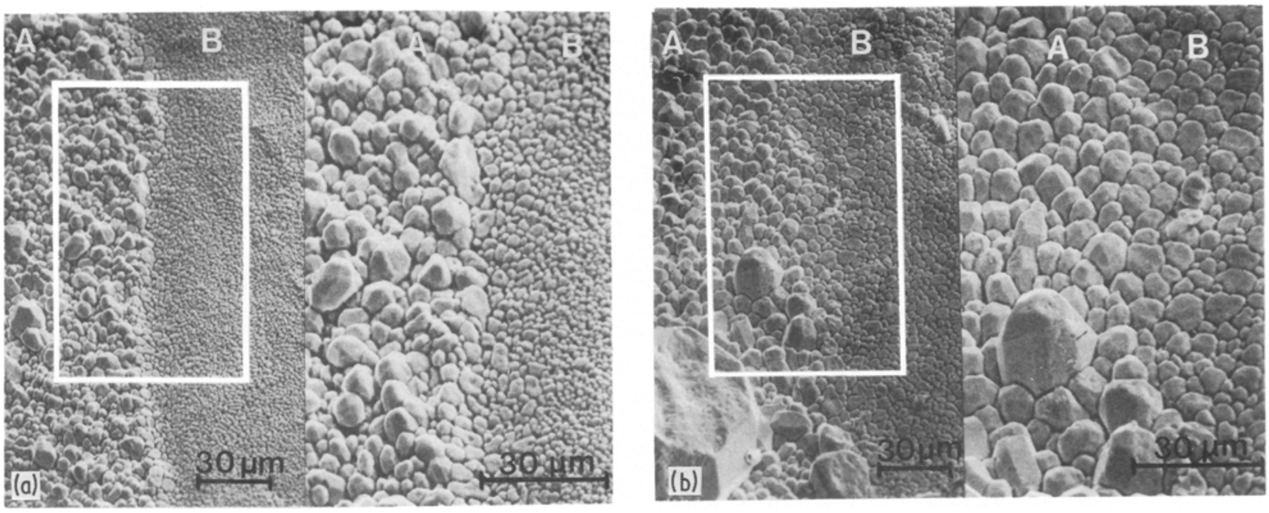

Figure 4 SEM micrographs showing the surface of an amalgamated silver disc 5 h after mounting in the SEM; (a) annealed at 60° C for 112 h, (b) annealed at 90° C for 112 h. There are grain-size and shape differences between the mercury-contacted Region A and the Teflon-masked Region B.

without determining the so-called Matano interface in the concentration penetration profile. The interdiffusion coefficient $\bar{D}$ at a certain mole fraction N_2 for the i phase which is formed between the initial mole fractions of N_2^- and N_2^+ is

$$\bar{D}(N_2) = \frac{1}{2t(\partial N_2/\partial x)}\left(\frac{N_2^+ - N_2^i}{N_2^+ - N_2^-} \times \int_{-\infty}^{x(i-1,i)} \frac{V_m^i}{V_m}(N_2 - N_2^-)\,\mathrm{d}x + \frac{(N_2^i - N_2^-)(N_2^+ - N_2^i)}{N_2^+ - N_2^-}\Delta x^i + \frac{N_2^i - N_2^-}{N_2^+ - N_2^-} \times \int_{x(i,i+1)}^{\infty} \frac{V_m^i}{V_m}(N_2^+ - N_2)\,\mathrm{d}x\right) \tag{1}$$

where t is the reaction time in sec. V_m^i is the molar volume of Phase i comprising $(1 - N_2^i)$ mol of Component 1 and N_2^i mol of Component 2, x is the distance from an arbitrary plane of reference, $x(i - 1, i)$ is the distance of the interface between Phases $(i - 1)$ and i, $x(i, i + 1)$ is the distance of the interface between Phases i and $(i + 1)$, Δx^i is the width of Phase i, expressed as $x(i, i + 1) - x(i - 1, i)$, and N_2^i is the average mole fraction of Component 2 in phase i.

In Equation 1 it is very difficult to determine local values of $\partial N_2/\partial x$ when the intermetallic compound i exists only in a narrow composition range. Equation 1 is therefore converted to the integral form below, to estimate the integral diffusivity in the homogeneity range of Phase i with limiting mole fractions $N_2^{i'}$ and $N_2^{i''}$ and the corresponding distances $x(i - 1, i)$ and $x(i, i + 1)$:

$$\int_{N_2{}^{i'}}^{N_2{}^{i''}} \bar{D}\,\mathrm{d}N_2 = \frac{(N_2^i - N_2^-)(N_2^+ - N_2^i)}{N_2^+ - N_2^-}\left(\frac{\Delta x^{i^2}}{2t}\right) + \frac{\Delta x^i}{2t}\left(\frac{N_2^+ - N_2^i}{N_2^+ - N_2^-}\int_{-\infty}^{x(i-1,i)} \frac{V_m^i}{V_m}(N_2 - N_2^-)\,\mathrm{d}x + \frac{N_2^i - N_2^-}{N_2^+ - N_2^-}\int_{x(i,i+1)}^{\infty} \frac{V_m^i}{V_m}(N_2^+ - N_2)\mathrm{d}x\right) \tag{2}$$

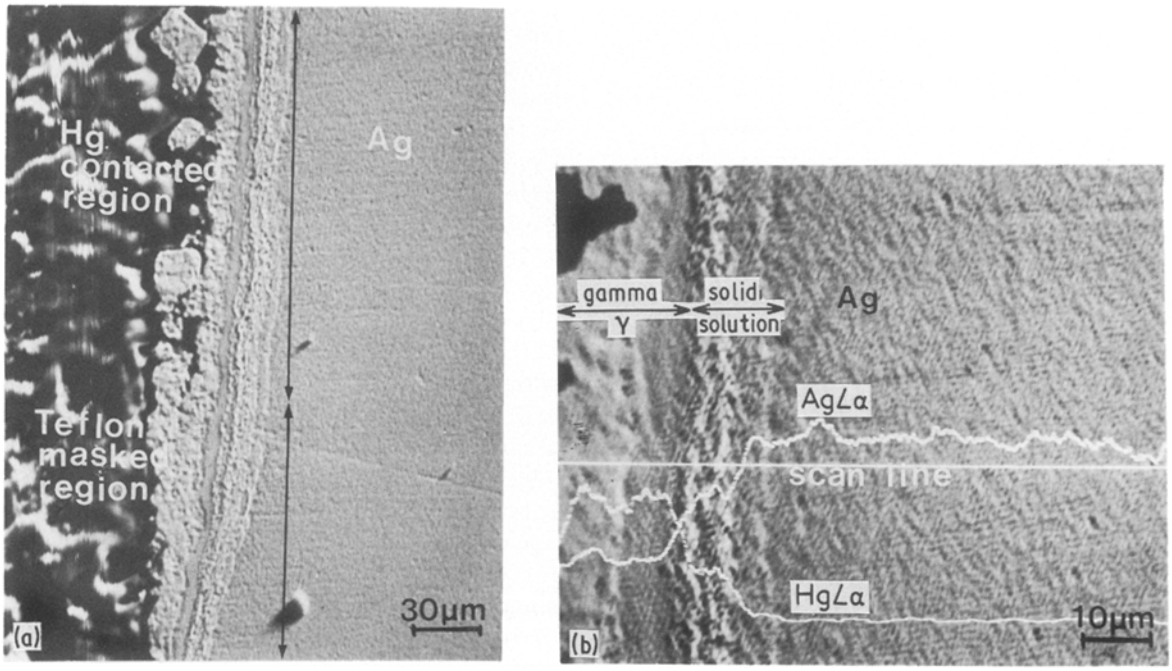

Figure 5 (a) Sectional view of Hg–Ag couple annealed at 115° C for 16 h, (b) X-ray line scans.

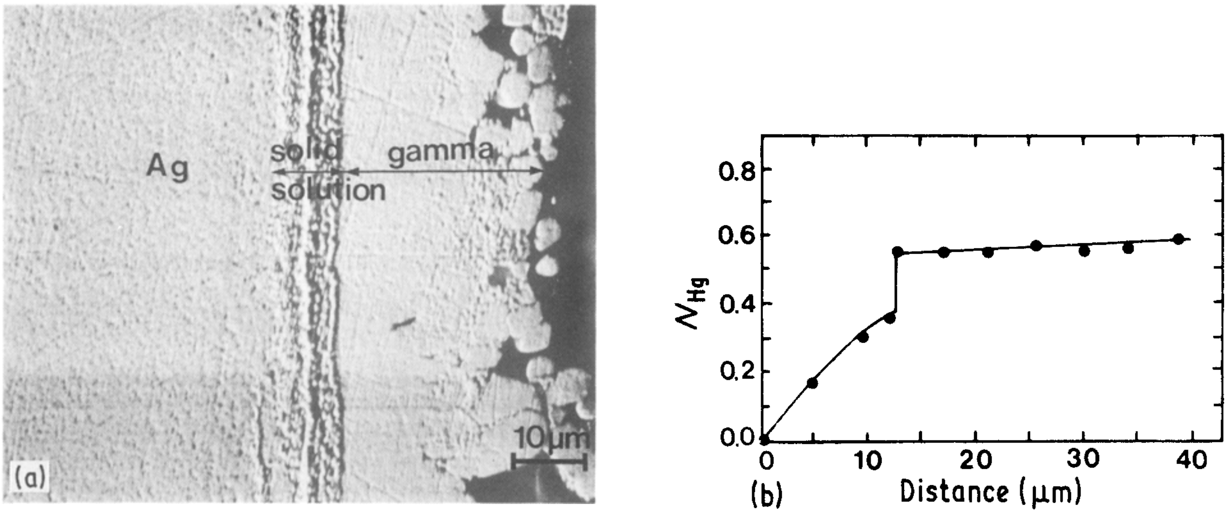

Figure 6 (a) Sectional view of Ag–Hg couple annealed at 40° C for 120 h, (b) concentration penetration curve of mercury for this couple.

Dividing Equation 2 by $(N_2^{i''} - N_2^{i'})$, the average interdiffusion coefficient D_{av} can be calculated as

$$D_{\mathrm{av}} = \frac{1}{N_2^{i''} - N_2^{i'}} \int_{N_2{}^{i'}}^{N_2{}^{i''}} \bar{D}\,\mathrm{d}N \tag{3}$$

In our system where pure Metal 1 and pure Metal 2 ($N_2^- = 0$, $N_2^+ = 1$) are used, Equation 2 is simplified as

$$\int_{N_2{}^{i'}}^{N_2{}^{i''}} \bar{D}\,\mathrm{d}N = N_2^i(1 - N_2^i)k_{\mathrm{I}}^i + \frac{\Delta x^i}{2t}\Bigg((1 - N_2^i) \times \int_{-\infty}^{x(i-1,i)} \frac{V_{\mathrm{m}}^i}{V_{\mathrm{m}}} N_2 \mathrm{d}x + N_2^i \int_{x(i,i+1)}^{\infty} \frac{V_{\mathrm{m}}^i}{V_{\mathrm{m}}}(1 - N_2)\,\mathrm{d}x\Bigg) \tag{4}$$

where k_{I}^i is the parabolic rate constant of the first kind for formation of Phase i, expressed as $(\Delta x^{i^2}/2t)_{N_2^- = 0, N_2^+ = 0}$.

From the slope of the straight lines in Fig. 7, k_{I}^i is calculated. The integral from $-\infty$ to $x(i - 1, i)$ in Equation 4 corresponds to that of the concentration profile of the solid-solution range in our system, and the integral from $x(i,\ i + 1)$ to $+\infty$, the liquid-mercury range. Since the concentration penetration curve for liquid mercury cannot be obtained in these experiments, it is assumed that the concentration gradient in liquid mercury is so small that the integral from $x(i,\ i + 1)$ to $+\infty$ is negligible. The other term, $-\infty$ to $x(i - 1, i)$, is calculated by graphical integration of the concentration penetration curve. The molar volume V_{m} in Equation 4 is estimated from lattice parameter data in the JCPDS X-ray file [8–10]. V_{m} changes linearly with concentration as shown in Fig. 8. The linear regressed equation for V_{m} is $V_{\mathrm{m}} = 10.361 + 27.84N_{\mathrm{Hg}}$, where N_{Hg} is the mole fraction of mercury in silver. A representative concentration penetration curve used in the calculation is given in Fig. 6b. The interdiffusion coefficients thus obtained are in Table I and the Arrhenius plot at 56 at % Hg is shown in Fig. 9 and represented as

$$D_{\mathrm{av}}(\mathrm{cm^2\,sec^{-1}}) = 3.181 \times 10^{-5} \exp(-32\,539\ (\mathrm{J\,mol^{-1}})/RT)$$

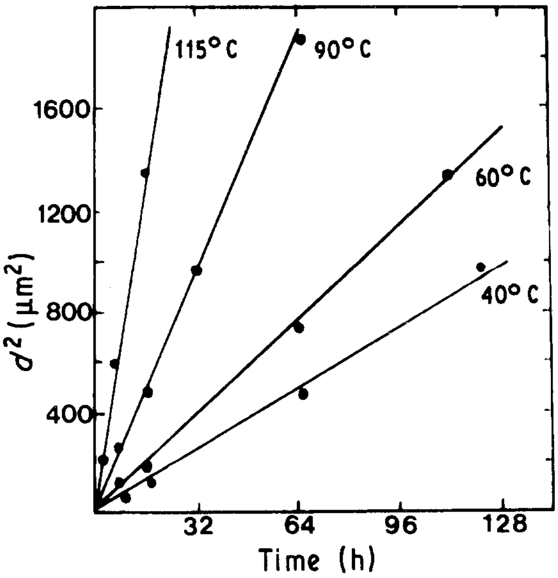

Figure 7 Plot of the square of the layer width of gamma phase against diffusion time in Ag–Hg couples.

4. Discussion

The low values of the frequency factor and activation energy for the parabolic growth of the gamma phase indicate the possibility of short-circuit diffusion through the gamma layer as in the Fe(s)–Sn(l) system [11]. As pointed out by van Loo and Rieck [12], the parabolic growth of the gamma layer is not in contradiction with a short-circuit mechanism, provided that the layer thickness is much larger than the distances between dislocations or grain boundaries. In this study, the very small grain size of gamma may be another indication of intermetallic growth of gamma by grain-boundary diffusion in the Hg–Ag contact reaction.

In dental amalgam, the mechanism of the

TABLE I Interdiffusion coefficients for gamma phase at various compositions and temperatures

Temperature (° C)	Time (h)	$D_{\mathrm{av}}(\mathrm{cm^2\,sec^{-1}})$	
		56 at % Hg	57 at % Hg
40	120	1.451×10^{-10}	1.441×10^{-10}
60	112	2.128×10^{-10}	2.114×10^{-10}
90	24	5.544×10^{-10}	5.499×10^{-10}
115	24	15.81×10^{-10}	15.71×10^{-10}

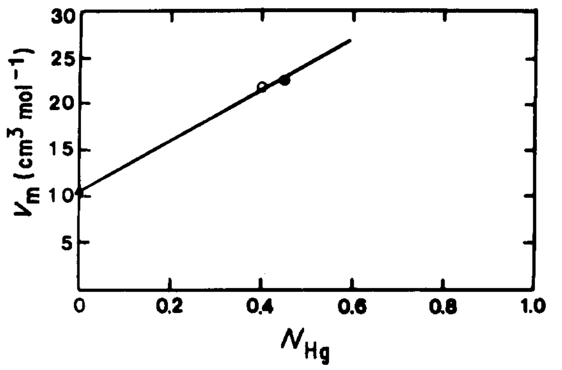

Figure 8 Molar volume V_m as a function of composition for the Ag–Hg system. (●) Schachnerite ($Ag_{1.1}Hg_{0.9}$), (○) *para*-schachnerite ($Ag_{1.2}Hg_{0.8}$).

amalgamation reaction has been believed to involve the dissolution of some of the Ag–Sn–Cu particles and the subsequent nucleation of the product phases from liquid Hg–Ag–Sn [13–18]. In the Ag–Hg system, however, the formation of product phase was caused by the diffusion of mercury into the silver matrix. As shown in the box of Fig. 4b, gamma crystals could grow towards liquid mercury only on a microscopic scale, but a gamma crystal layer in the silver matrix (as shown in the sectional view of the diffusion couple in Figs. 5a and 6a) was increased as the reaction time and temperature were increased. These gamma crystals were found to be easily crumbled off in the liquid mercury. This crumbling-off phenomenon may also occur in real dental amalgam. The crumbling-off phenomenon of this phase should be considered in the interpretation of the reaction mechanism. The penetration of mercury into the grain boundary of the gamma layer causes the gamma crystals to be easily crumbled off, and these crystals may be mistaken for crystals which have been precipitated in the liquid mercury by the solution precipitation mechanism.

The epsilon phase (generally designated as beta) was not found in the couple annealed for at least 120 h in the temperature range 40 to 60° C, though as the temperature and annealing time were increased a very small globular epsilon phase was found in the solid solution of Ag–Hg. The epsilon phase was not therefore considered in the calculation of D_{av} in gamma for the range of temperature and time in this study. The extra phase which was claimed to exist by Suprinick [4] was not found in this research. He insisted on the presence of four intermediate phases in a diffusion couple annealed at 93.3° C. The method of phase identification he employed was optical microscopy, and he did not given any evidence for their existence. As shown in Fig. 5, the morphology of the reaction product is very likely to induce misinterpretation of the reaction products.

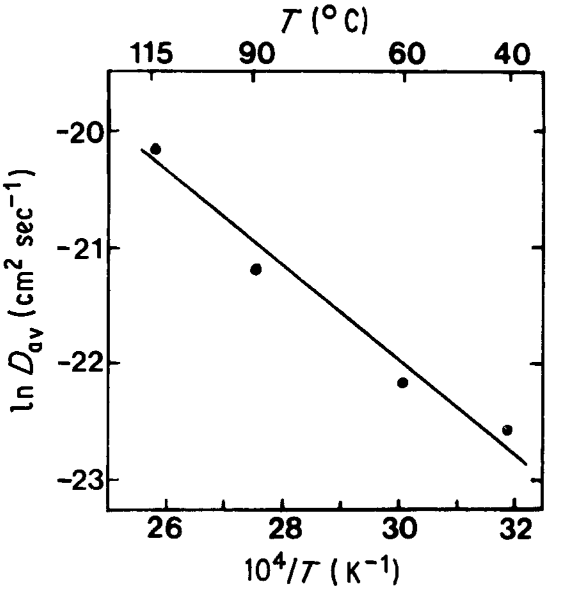

Figure 9 Plot of lnD_{av} against $1/T$ for the reaction layer in an Ag–Hg couple between 40 and 115° C.

5. Conclusions

The amalgamation reaction between silver and liquid mercury at temperatures ranging from 40 to 115° C proceeded with the formation of gamma phase (the range of composition is 55.3 to 57.5 at % Hg), and a solid solution of Ag–Hg. The growth of gamma phase followed a parabolic rate law. The average interdiffusion coefficient was found to be $D_{av}(\text{cm}^2\,\text{sec}^{-1}) = 3.181 \times 10^{-5} \exp(-32\,539\ (\text{J mol}^{-1})/RT)$ in the temperature range between 40 and 115° C. The low values of the activation energy as well as the frequency factor indicated the important role of grain-boundary diffusion through the gamma layer in this system. The penetration of liquid mercury into the grain boundary of gamma caused the gamma to be crumbled off. The suggested unknown phase which was claimed to exist by Suprinick [4] was not found in this research.

References

1. M. L. MALHOTRA, C. L. REYNOLDS and R. E. BARKER, *J. Chem. Phys.* **10** (1974) 3831.
2. T. OKABE, A. L. HINES and R. F. HOCHMAN, *J. Appl. Phys.* **1** (1976) 49.
3. A. SAWATZKY and F. E. JAUMOT, *Trans. AIME* **10** (1957) 1207.
4. H. SUPRINICK, *J. Dent. Res.* **50** (1971) 944.
5. J. R. ABBOTT and O. F. MAKINSON, *ibid.* **57** (1978) 790.
6. M. HANSEN, "Constitution of Binary Alloys" (McGraw-Hill, New York, 1958) p. 25.
7. G. WAGNER, *Acta Metall.* **17** (1969) 99.
8. "Selected Powder Diffraction Data" (JCPDS, International Center for Diffraction Data, Swarthmore, 1978) p. 147.
9. "Selected Powder Diffraction Data" (JCPDS, International Center for Diffraction Data, Swarthmore, 1978) p. 914.
10. C. P. HEIJWEGEN and G. J. VISSER, *Scripta Metall.* **7** (1973) 223.
11. J. A. van BEEK, S. A. STOLK and J. J. van LOO, *Z. Metallkde* **73** (1982) 439.
12. F. J. J. van LOO and G. D. RIECK, *Acta Metall.* **21** (1973) 61.
13. C. L. REYNOLDS, Jr, F. E. WAWNER and H. G. WILSDORF, *J. Appl. Phys.* **2** (1975) 568.
14. T. OKABE, R. MITCHELL, M. B. BUTTS, A. H. WRIGHT and C. W. FAIRHURST, *J. Dent. Res.* **7–8** (1978) 759.
15. T. OKABE and R. F. HOCHMAN, *J. Biomed. Mater. Res.* **9** (1975) 221.
16. T. OKABE, A. L. HINES and R. F. HOCHMAN, *ibid.* **9** (1975) 389.
17. P. G. BOSWELL, *J. Mater. Sci. Lett.* **15** (1980) 1311.
18. J. M. DUBOIS, G. Le CAER, B. BERNARD, J. G. DUMAGNY and F. DUPONT, *Acta Metall.* **29** (1981) 1159.

Received 3 July
and accepted 18 September 1985